TITLE: Inhibition of plasminogen/plasmin system retrieves endogenous nerve growth factor and adaptive spinal synaptic plasticity following peripheral nerve injury

AUTHORS: Assunta Virtuoso[a, 1], Anna Maria Colangelo[b, e, 1], Sohaib Ali Korai[a], Sara Izzo[a], Antonio Todisco[a], Roberto Giovannoni[c], Marialuisa Lavitrano[d, 2], Michele Papa[a, e, 2], Giovanni Cirillo[a, 2]

AFFILIATIONS:

[a] Division of Human Anatomy, Laboratory of Morphology of Neuronal Networks, Department of Mental and Physical Health and Preventive Medicine, University of Campania "Luigi Vanvitelli, Naples, Italy

[b] Laboratory of Neuroscience "R. Levi-Montalcini", Dept. of Biotechnology and Biosciences, University of Milano-Bicocca, Milano, Italy

[c] Department of Biology, University of Pisa, Italy

[d] School of Medicine and Surgery, University of Milano-Bicocca, Monza, Italy

[e] SYSBIO Centre of Systems Biology ISBE.ITALY, University of Milano-Bicocca, Milano, Italy

Correspondence to:

Giovanni Cirillo & Michele Papa, Division of Human Anatomy, Laboratory of Morphology of Neuronal Networks Department of Mental, Physical Health and Preventive Medicine University of Campania "Luigi Vanvitelli", via L. Armanni, 5, 80138, Naples, Italy.

FOOTNOTES: [1] co-first authorship, [2] co-last authorship

Abstract

Dysfunctions of the neuronal-glial crosstalk and/or impaired signaling of neurotrophic factors represent key features of the maladaptive changes in the central nervous system (CNS) in neuroinflammatory as neurodegenerative disorders. Tissue plasminogen activator (tPA)/plasminogen (PA)/plasmin system has been involved in either process of maturation and degradation of nerve growth factor (NGF), highlighting multiple potential targets for new therapeutic strategies.

We here investigated the role of intrathecal (i.t.) delivery of neuroserpin (NS), an endogenous inhibitor of plasminogen activators, on neuropathic behavior and maladaptive synaptic plasticity in the rat spinal cord following spared nerve injury (SNI) of the sciatic nerve.

We demonstrated that SNI reduced spinal NGF expression, induced spinal reactive gliosis, altering the expression of glial and neuronal glutamate and GABA transporters, reduced glutathione (GSH) levels and is associated to neuropathic behavior. Beside the increase of NGF expression, i.t. NS administration reduced reactive gliosis, restored synaptic homeostasis, GSH levels and reduced neuropathic behavior.

Our results hereby highlight the essential role of tPA/PA system in the synaptic homeostasis and mechanisms of maladaptive plasticity, sustaining the beneficial effects of NGF-based approach in neurological disorders.

1. INTRODUCTION

Morpho-functional changes of neuro-glial network after peripheral nerve injury (PNI) lead to the establishment of a maladaptive synaptic plasticity in the central nervous system (CNS) (Kim et al., 2017; Papa et al., 2014; Virtuoso et al., 2020). This process begins with the activation of glial cells (reactive astrocytes and microglia), boosting the release of a variety of cytokines, proinflammatory mediators and amino acidic neurotransmitters, altering the expression of glutamatergic and GABAergic receptors and transporters (West et al., 2015), inducing central (De Leo et al., 2006) and peripheral sensitization (Papa et al., 2014; Virtuoso et al., 2019). Altogether, the maladaptive changes after PNI impair the neuron-astrocyte crosstalk, thus contributing to an altered homeostasis in the spinal cord, neuroinflammatory reactions and neurodegeneration. Moreover, pain transmission is enhanced and characterized by allodynia and hyperalgesia, two distinctive aspects of the chronic neuropathic pain (Gwak et al., 2017; Kuner and Flor, 2016). We have previously demonstrated new mechanisms and potential therapeutic applications of nerve growth factor (NGF) (Cirillo et al, 2010, 2011) and its homologue synthetic peptide BB14 (Cirillo et al., 2012; Colangelo et al., 2008) in a rat model of PNI. We reported that intrathecal (i.t.) NGF and its homologue synthetic NGF-like peptide BB14 showed anti-inflammatory and anti-gliosis effects in the spinal cord after spared nerve injury (SNI) of the sciatic nerve, restoring the glial uptake of neurotransmitters, the neuro-glial homeostasis, and reducing the maladaptive synaptic plasticity (Cirillo et al., 2012). These changes were paralleled by significant reduction of the chronic neuropathic pain.

Experimental and clinical reports unequivocally correlate the coagulation system with the maladaptive synaptic plasticity, neuroinflammatory and degenerative disorders of the CNS (De Luca et al., 2018; Merlini et al., 2019). Evidence has demonstrated that endogenous NGF levels are regulated by the activity of the metalloproteinase-9 (MMP-9), a constitutive proteinase in CNS

activated by the tissue plasminogen activator (tPA)/plasminogen (PA)/plasmin system (Bruno and Cuello, 2006). We demonstrated that the inhibition of NGF degradation and the consequent increase of its endogenous contents by i.t. administration of the metalloproteinases (MMPs) inhibitor GM6001 had the same effect on the spinal maladaptive plasticity compared to the exogenous NGF administration (Cirillo et al., 2012). GM6001 restored the endogenous NGF content, reduced the reactive gliosis and rescued neuro-glial homeostasis and neuropathic pain behavior (Osikowicz et al., 2013) in the spinal cord after sciatic SNI (Virtuoso et al., 2020). The tPA/PA/plasmin/MMPs system could be also modulated by neuroserpin (NS), a family member of the serine proteinase inhibitors, known to be the endogenous inhibitor of tPA and urokinase plasminogen activator (uPA) in the brain (Krueger et al., 1997; Lee et al., 2015, 2017). NS is constitutively expressed in the developing brain (Adorjan et al., 2019; Kement et al., 2021) and is required for neurite outgrowth (Par- mar et al., 2002), refinement of synapses (dendritic branching, spine morphology) and normal synaptic plasticity (Reumann et al., 2017). NS has neuroprotective effects against oxidative stress, microglia-mediated inflammatory response (Yang et al., 2016) and cell death in primary culture of hippocampal neurons (Cheng et al., 2017) and astrocytes (Wang et al., 2015). NS-deficient mice show an excessive microglial activation (Gelderblom et al., 2013), while NS promotes functional recovery in several animal models after acute spinal cord (Li et al., 2018) and vascular brain injury (Li et al., 2017). NS-induced inhibition of tPA blocks the conversion of PA into plasmin that ultimately has two main functions: 1) activation of MMP-9 (from the pro-enzyme to the mature, active form) and 2) conversion of proNGF (the precursor of NGF) into mature NGF (Bruno and Cuello, 2006).

We aim to evaluate the effects of i.t. NS delivery to SNI rats on spinal reactive gliosis, neuro-glial homeostasis, maladaptive plasticity and neuropathic behavior.

2. MATERIALS AND METHODS

2.1. Animals and SNI model

Male adult (250–300 g) Sprague Dawley rats (n 24) (Charles River, Italy) were used for all experiments, maintained on a 12/12 h light/dark cycle, allowed free access to food and water. SNI of the sciatic nerve was made according to the methods previously described (Cirillo et al., 2011; Decosterd and Woolf, 2000). Briefly, animals were anesthetized with intraperitoneal (i.p.) chlorydrate tiletamine (30 mg/kg), the right sciatic nerve exposed and the tibial and common peroneal nerves ligated and axotomized, leaving the sural nerve intact. In sham-operated control animals (CTR), sciatic nerve was exposed but not truncated. All surgery and experimental procedures were approved by the Ethics Committee of the University of Campania "Luigi Vanvitelli". Animal care was in compliance with the Italian and European Guidelines for use and care of laboratory animals (EU Directive 2010/63).

2.2. Drug delivery

Local NS treatment has been suggested to be beneficial in neurological disorders (Cinelli et al., 2001). Based on this evidence, an i.t. lumbar spinal catheter [polyethylene (PE) 10 tube attached to PE 60 tube for connection to an osmotic pump] was inserted through the subarachnoid space toward the lumbar spinal cord during the SNI surgery and anchored to the vertebral bones by glass ionomer luting cement (Ketac Cem radiopaque; 3M ESPE, Germany). Three-days after SNI, rats were anesthetized by i.p. chlorydrate tiletamine (30 mg/kg), the free extremity of the spinal catheter was connected to an osmotic minipump (Alzet, mod. 2001, Cupertino, CA), filled with NS (Abnova, Taiwan) (0.05 μg/μl, corresponding to 30 μg/kg) or vehicle only (artificial cerebrospinal fluid, ACSF) and implanted subcutaneously. The pump rate was 1 μl/h for 7 days, thus producing an i.t. infusion dose of 0.05 μg/μl/h of NS. The chronic treatment was preferred since NS appears to function as a transient inhibitor of tPA in vivo (Lee et al., 2015).

2.3. Behavioral testing

Animals were tested on day 0 (before SNI and lumbar spinal catheter positioning), day 3 (3 days after SNI), and day 10 (7 days after treatment), when all animals were sacrificed. Mechanical allodynia was assessed by the von Frey filament test (Ugo Basile) (Chaplan et al., 1994; Yamanaka et al., 2016). Filaments were applied under the plantar surface of the right paw in the sural region, in either ascending or descending strength as necessary to determine the filament closest to the threshold of response. The time of response to a progressive force applied to hind paw limb (30g in 20 s) was evaluated six times, with an interval of 5 min between stimulations. The threshold was the lowest force that evoked a consistent, brisk, withdrawal response.

Nociceptive thresholds to radiant heat (infra-red) were measured using the plantar test apparatus (Ugo Basile) (Hargreaves et al., 1988). The heat source was positioned under the plantar surface of the right hind paw and activated at a setting intensity of 7.0 to record the response latency for paw withdrawal. A cut-off time of 20 s was imposed to prevent tissue damage. The injured hind limb was tested twice at each time point, with an interval of 5 min between stimulations. All testing was performed blind.

2.4. Tissue preparation and spinal cord immunohistochemistry

Rats were deeply anesthetized by i.p. injection of chloral hydrate 4% (300 mg/kg body weight) and perfused transcardially with saline solution (Tris HCl 0.1M/EDTA 10 mM) followed by 4% paraformaldehyde added to 0.1% glutaraldehyde in 0.01 M phosphate-buffer (PB), pH 7.4 at 4◦C. Spinal cords were removed and post-fixed 2 h in the same fixative, then soaked in 30% sucrose PBS and frozen in chilled isopentane on dry ice. Serial sections (25 µm thickness) were cut at the slide microtome and collected in cold PBS for immunohistochemistry (IHC).

The following antibodies were used for IHC: mouse antibodies directed against Glial Fibrillary Acidic Protein (GFAP) (1:400; Sigma-Aldrich Milano, Italy); rabbit antibodies to ionized calcium binding adaptor molecule 1 (Iba1) (1:500; Wako Chemicals, USA); guinea pig antibodies to glutamate transporter (GLT1) (1:200; Chemicon Inc Temecula, CA, USA); goat antibodies to glycine transporter 1 (GlyT1) (1:1000; Chemicon Inc Temecula, CA, USA); guinea pig antibodies raised against vesicular glutamate transporter 1 (vGLUT1) (1:5000; Chemicon Inc Temecula, CA, USA); mouse antibodies to vesicular GABA transporter (vGAT) (1:500; Synaptic Systems, Gottingen, Germany); rabbit antibodies against Glutamic Acid Decarboxylase 65/67 (GAD65/ 67) (1:1000; Sigma-Aldrich, Milano, Italy); goat antibodies to neuronal glutamate carrier EAAC1 (1:4000; Chemicon Inc Temecula, CA, USA); rabbit antibodies against NGF (1:250; Chemicon Temecula, CA, USA); rabbit antibodies against proNGF (1:250; Sigma-Aldrich, Milano, Italy). Spinal cord sections were blocked in 10% normal serum in 0.01M PBS/0.25% Triton-X100 for 1 h at room temperature (RT). Each primary antibody (GFAP, Iba1, GLT1, GlyT1, EAAC1, NGF, proNGF) was diluted in 0.01 M PBS containing 10% normal serum and 0.25% Triton. Following incubation for 48 h at 4◦C, sections were washed several times in PBS and incubated with the appropriate biotinylated secondary antibody (Vector Labs Inc., Burlingame, CA, USA; 1:200) for 90 min at RT, washed in PBS and processed using the Vectastain avidin-biotin peroxidase kit (Vector Labs Inc., Burlingame, CA, USA) for 90 min at RT. Sections were then washed in 0.05 M Tris-HCl and reacted with 3.3-diaminobenzidine tetrahydrochloride (DAB; Sigma, 0.5 mg/ml in Tris-standard samples [glutamic acid, glutamine, glycine and gamma- aminobutyric acid (GABA), 0.25 mM each]. Method reproducibility was assessed by analyzing all samples for five consecutive times. Aminoacidic concentrations were expressed as the mean of the peak areas, and the standard error of the mean (SEM) and coefficient of variation (% CV) were calculated. Results were reported as the ratio between the percentage of the areas versus the total area of the investigated amino acids.

155 2.7. Measurements and statistical analysis

156 Slides were imaged with a Zeiss Axioskope 2 light microscope equipped with high-resolution digital
157 camera (C4742-95, Hamamatsu Photonics, Italia). Measurements of markers in the dorsal horn of
158 spinal HCl) and 0.01% hydrogen peroxide. Sections were mounted on cords were performed using
159 computer assisted image analysis system chrome-alume gelatine coated slides, dehydrated and
160 coverslipped. Immunofluorescence staining was performed as described previously (Papa et al.,
161 2003). Sections were incubated with the primary antibody (vGLUT1, vGAT and GAD65/67) for 48 h
162 at 4◦C. Following incubation with primary antibodies, sections were incubated with the
163 appropriate secondary antibody (Alexa Fluor 488 anti-guinea pig IgG, Alexa Fluor 488 anti-mouse
164 IgG, Alexa Fluor 546 anti-rabbit IgG and Alexa Fluor 488 anti-rabbit IgG) (1:200; Invitrogen,
165 Carlsbad, CA) for 2 h. Sections were mounted and coverslipped with Vectashield (Vector
166 Laboratories) and acquired by the Zeiss LSM 510 Meta laser scanning microscope (Oberkochen,
167 Germany). Confocal images of dorsal horns of lumbar spinal cord were captured at a resolution of
168 512x512 pixels. The Argon laser fluorescence was used for visualization of the vGLUT1 and vGAT
169 (excitation wavelength of 488 nm and emission filter bandpass 505–530 nm), the HeNe laser
170 fluorescence was used for the GAD65/67 signal (excitation wavelength of 546 nm and emission
171 filter long-pass 560 nm).

172 2.5. MMPs activity and GSH assays

173 In situ zymography was performed to evaluate the gelatinolytic activity in the lumbar spinal cord
174 (EnzCheck Gelatinase Assay Kit; Molecular Probes). Frozen sections (25 µm thick) were incubated
175 with DQ gelatin conjugate, the fluorogenic substrate, at 37◦C overnight and, after washing, fixed in
176 4% paraformaldehyde in PBS. Cleavage of DQ gelatin by proteases resulted in a green fluorescent
177 product and was analyzed by confocal microscopy. Gelatinase MMPs activity was evaluated with
178 the HeNe laser (excitation 546 nm, emission filter long-pass 560 nm). For GSH assay, spinal cord

sections were incubated overnight in ACSF containing 40 µM of monochlorobimane (MCB), a thiol reactive reagent and then transferred to fresh ACSF for 30 min. Slides were fixed in 4% paraformaldehyde and then analyzed by confocal microscopy. GSH levels were analyzed with a UV laser (excitation 351 nm, emission 364 nm).

2.6. HPLC analysis

Amino acids levels were analyzed by RP-HPLC analysis using an Agilent 1200 Series Liquid Chromatograph, equipped with a binary pump delivery system (G1312B), robotic autosampler (G1317B), column thermostat (G1316A) and multi-wavelength detector (G1315B). Briefly, tissues samples were diluted in borate buffer (0.15 M, pH 10.2) followed by addition of the derivatization solution [o-Phthalaldehyde (OPA) (10 mg/ml), β-mercaptoethanol (10 mg/mL)] and diluent solution (mobile phase A: 1.5% v/v H3PO4). After derivatization, the mixture (20 µl) was injected on a reverse-phase Jupiter 5 µm C18 300 Å (250 mm 4.6 mm) column at 40◦C and derivatives absorption detected at 338 nm. Separation was obtained at a flow rate of 1 mL/min with a gradient of the mobile phase A [Na2HPO4 (10 mM)/ Na2B4O7.10 H2O (10 mM)], and phase B [methanol:acetonitrile:water (9:9:2, v:v:v)]. Spinal cord samples were automatically derivatized by the robotic autosampler and analyzed blindly by using amino acid (MCID 7.0; Imaging Res. Inc, Canada). Glial markers (GFAP and Iba1) and in situ zymography were analyzed through a morphometric approach and expressed as a proportional area (number of positive elements relative to the scanned area). Densitometric values were re- ported for GLT1, GlyT1, EAAC1, NGF and proNGF (total density within the target outline multiplied by its area) and also for the analysis of confocal images for vGLUT1, vGAT, GAD65/67 and GSH. Averages were obtained from five randomly selected spinal cord sections for each animal, and comparisons were made between treatment (NS) versus control groups (ACSF and CTR). Data were exported and converted to frequency distribution histograms by using the Sigma- Plot 10.0 program (SPSS Erkrath Germany).

Data from all the quantitative analyses were analyzed by one-way ANOVA, using all pairwise Holm-Sidak method for multiple comparisons (*p 0,01; **p 0.001). All data shown are presented as the mean±SEM. Individual images of control and treated rats were assembled and then the same adjustments were made for brightness, contrast and sharpness using Adobe Photoshop (Adobe Systems, San Jose, CA).

3. RESULTS

3.1. NS-induced modulation of endogenous NGF and proNGF expression in the spinal cord after SNI

To verify the efficacy of NS in the inhibition of the tPA/PA/plasmin/ MMPs/NGF axis, we first evaluated the endogenous NGF and proNGF expression in the rat dorsal spinal cord. Immunohistochemical analyses revealed that endogenous NGF levels were reduced in the ACSF group (18.37±3.14), compared to CTR animals (41.23±2.49) (Fig. 1A). The reduction of NGF content in SNI animals was counterbalanced by a significant increase of the proNGF levels (43.24±2.97), compared to CTR animals (22.85±3.16) (Fig. 1B). The NS-induced inhibition of the tPA/PA/plasmin system blocked the conversion of proNGF into mature NGF and inhibited the NGF degradation via MMP-9. Accordingly, i.t. treatment with NS for 7 days following PNI increased endogenous NGF expression (33.46±2.43) and reduced proNGF levels (28.11±3.45) (Fig. 1B) in the dorsal horn of lumbar spinal cord (**p 0.001, NS vs ACSF).

In situ zymography of lumbar spinal cord sections revealed a significant increase of the gelatinolytic activity in ACSF-treated animals (17.5±0.3), as compared to CTR animals (11.2±0.6). The specific inhibitory effect of NS on the proteolytic activity of the MMP2 and MMP9 was confirmed by the strong reduction of the gelatinolytic activity in the NS group (8.2±0.2), as

compared to ACSF animals (Fig. 1C) (**p≤0.001, NS vs ACSF). These results confirmed the efficacy of NS in reducing the activity of MMPs, thus increasing the levels of endogenous NGF.

3.2. NS-induced reduction of reactive gliosis after PNI

SNI induced significant reactive gliosis in the dorsal horn of lumbar spinal cord as expressed by the strong increase of GFAP (18.62±0.79) (Fig. 2A) and Iba1 levels (4.75±0.31) (Fig. 2B) in the ACSF-treated animals compared to the values in CTR group (GFAP: 9.24±0.29; Iba1: 1.33±0.24) (**p≤0.001, ACSF vs CTR). I.t. administration of NS for 7 days significantly reduced both GFAP (9.62±0.34) and Iba1 (2.83±0.25) expression levels, as compared to ACSF-treated SNI rats (Fig. 2) (**p≤0.001, NS vs ACSF).

Altogether, these data support a NGF-mediated role of NS in reducing reactive astrocytosis and microglial recruitment after SNI.

3.3. Modulation of spinal synaptic homeostasis by i.t. NS administration

We evaluated the expression of the glial glutamate and glycine transporters (GGTs) after SNI and after i.t. delivery with NS for 7 days. The expression of the main astrocytic glutamate transporter GLT1 in the dorsal horn spinal cord was reduced after SNI (4.17±0.49), compared to the CTR group (7.79±0.51) (Fig. 3A). In SNI animals, we also observed a significant reduction of the glycine transporter (GlyT1) (4.91±0.59), compared to CTR animals (7.88±0.19) (Fig. 3B). Reduction of GLT1 in the ACSF group was counterbalanced by an increased expression of the neuronal glutamate transporter EAAC1 (45.46±3.93), compared to CTR animals (23.13±3.43) (Fig. 3C) (**p≤0.001, ACSF vs CTR). The reduction of glial glutamate uptake after SNI and the consequent extracellular glutamate increase was confirmed by HPLC analysis of the Glutamate/GABA ratio that was significant higher in ACSF treated animals (16.3±1.5) compared to CTR animals (5.7±1.4) (Fig. 4).

I.t. delivery of NS increased the expression levels of GLT1 (8.12±0.44), GlyT1 (6,96±0.43) and reduced the expression of EAAC1 (26,70±2.43) (Fig. 3) (**p≤0.001 NS vs ACSF), demonstrating that NS modulates the expression of glial as neuronal transporters in the dorsal spinal cord after SNI. In parallel to the increase of the GLT1 expression, NS treatment reduced the Glutamate/GABA ratio (8.9±0.8) (**p≤0.001, NS vs ACSF) (Fig. 4), highlighting its beneficial role in the modulation of neurotransmitters levels at the synaptic cleft.

To further characterize the mechanisms of synaptic homeostasis linked to reactive gliosis, we also analyzed vGLUT, vGAT and GAD65/67 expression in SNI rats. No significant changes were found in vGLUT levels between groups (CTR: 14.4±1.2; ACSF: 13.9±0.9; NS: 13.7±0.8) (Fig. 5A). In contrast, a net increase of vGAT staining was found in the dorsal horns of lumbar spinal cord of ACSF group (5.8±0.4), as compared to the CTR group (2.1±0.3) (Fig. 5B). A strong increase of GAD65/67 was also observed in 7-days ACSF-treated animals (18.9±0.74), as compared to the CTR group (8.7±1.32) (Fig. 5C). Interestingly, the beneficial effect of NS in reducing the MMPs activity and the glial reaction was paralleled by its modulation of neurotransmitter transporter expression. Indeed, immunofluorescence analysis of dorsal horns of lumbar spinal cord for vGAT and GAD65/67 revealed that NS treatment restored vGAT (2.0±0.3) and GAD65/67 (8.02±0.93) expression to CTR values (**p≤0.001 versus ACSF) (Fig. 5B–C) (**p≤0.001 NS vs ACSF).

3.4. Neuroprotective effect of NS

Synthesis and production of glutathione (GSH), one of the main neuronal antioxidant defenses, is strictly dependent on the availability of glutamate, glycine and cysteine, mainly taken up by astrocytic transporters. Due to the significant reduction of GGTs expression after SNI, we examined the GSH levels by confocal microscopy following MCB staining. We found a strong reduction of GSH levels in ACSF-treated rats (2.49±0.37), as compared to the CTR group (7.24±0.43) (Fig. 6). I.t. treatment with NS restored GSH levels (8.03±0.18) (**p≤0.001, NS vs

ACSF), strongly supporting the protective function of endogenous NGF against excitotoxicity and oxidative stress.

3.5. I.t. administration of NS reduces the neuropathic pain behavior in SNI rats

We tested the efficacy of NS on neuropathic behavior on days 0, 3, and 10 after SNI by analyzing mechanical and thermal sensitivity. The mean baseline mechanical and thermal thresholds before SNI (day 0) for all groups were 28.64±0.54 g and 16.18±0.60 s, respectively. In CTR animals these values were unmodified on day-3 (28.75±0.42 g and 16.20±0.41 s) and day-10 (28.54±0.35 g and 16.24±0.35 s), respectively (Fig. 7A). SNI induced a neuropathic behavior on day-3, as showed by the significant reduction of the mechanical threshold in ACSF (10.24±0.48 g) and NS-treated animals (11.84±0.42 g), indicative of an allodynic state. This condition was still evident on day-10, after 7 days of ACSF i.t. delivery (10.54±0.60 g). The Hargreaves test confirmed the onset of an hyperalgesic state on day-3 in SNI animals of ACSF (6.15±0.54 s) and NS (6.30±0.47 s) group that was still persistent 7 days later, after i.t. ACSF infusion (6.30±0.57 s) (Fig. 7B). I.t. administration of NS to neuropathic SNI animals for 7 days improved mechanical (22.84±0.35 g) and thermal sensitivity (12.84±0.43 s) (Fig. 7A–B) (**$p \leq 0.001$, NS vs ACSF), strongly suggesting that mechanisms underlying chronic pain may involve a decrease of NGF availability.

4. DISCUSSION

Our results demonstrate that PNI reduced spinal NGF expression, activated glial cells, altering the expression of glial and neuronal transporters, and reducing GSH levels. A crucial role is played by the tPA/PA/plasmin system involved in the metabolism of NGF, that in turn modulates glial activation, maintains synaptic homeostasis and restore maladaptive plasticity.

294 Modulation of spinal maladaptive synaptic plasticity, therefore, represents a valid strategy to
295 prevail synaptic dysfunction following PNI (Kuner and Flor, 2016; Lo´pez-Gonza´lez et al.,
296 2017). Spinal reactive gliosis represents one of the main components of the synaptic network
297 rearrangement after sciatic SNI. In this process, neurotrophins and NGF play a crucial role in
298 modulating mitochondrial function, restoring glial mechanisms of synaptic homeostasis,
299 neurogenesis, neuroregeneration (Martorana et al., 2018) and neuroprotection (Rizzi et al., 2018;
300 Sofroniew et al., 2002). Endogenous NGF levels are the result of the balance between protease-
301 dependent conversion of proNGF into mature NGF and protease-dependent NGF degradation
302 (Bruno and Cuello, 2006). In the dorsal spinal cord after SNI, in parallel with a reduction of
303 endogenous NGF, we reported an increase of proNGF expression, as a probable compensatory
304 mechanism to restore NGF levels (Fig. 1A–B). This result is in agreement with the reported
305 increase of proNGF after CNS injury, and its activity through the p75 and sortilin receptors
306 (Harrington et al., 2004; Nykjaer et al., 2004). Both the conversion of proNGF into NGF and NGF
307 degradation occur through the protease system of tPA/PA/plasmin/MMPs (Bruno and Cuello,
308 2006), the latest being overexpressed during neuro-inflammatory disorders (De Luca and Papa,
309 2016). As a result, we demonstrate a strong increase of the MMPs activity after SNI (Fig. 1C),
310 supporting our data regarding the NGF and proNGF expression.

311 NS is the inhibitor of tPA and uPA in the CNS and its activity directly modulates the NGF levels
312 blocking i) the production of plasmin, that is responsible for proNGF → NGF conversion; ii) the
313 activation of mature MMPs from precursor (proMMPs), that in turn degrade NGF. In particular,
314 tPA and uPA knockout mice have been reported to decrease the gelatinase proteases (MMP2 and
315 MMP9) activity (Siconolfi and Seeds, 2003). Accordingly, SNI animals were treated with i.t. NS and
316 presented a reduction of the gelatinolytic activity in the dorsal spinal cord, increased endogenous
317 NGF level and reduced proNGF expression (Fig. 1).

The NS-induced endogenous NGF increase prompted us to study the maladaptive plasticity in the spinal cord following SNI. In line with our previous works (Cirillo et al, 2011, 2012, 2015), we report a strong microglial and astrocytic reaction in the dorsal spinal cord after nerve injury, as showed by the increase of Iba1 and GFAP staining (Fig. 2). I.t. delivery of NS strongly reduces the reactive gliosis, thus paralleling the anti-gliotic effect of NGF. Recent studies have identified microglial cells as the target of NGF or NGF mimetics, that drive them toward a non-inflammatory phenotype (James et al., 2017; Rizzi et al., 2018).

Reactive gliosis induces profound changes in the neuron-astroglial neurotransmitters crosstalk. We here confirm the significant reduction of glial glutamate (GLT1) and glycine (GlyT1) transporters, the increase of the neuronal glutamate transporter EAAC1 (Fig. 3) and vesicular GABA transporters (Fig. 5). These data further correlate to the increase of the Glutamate/GABA ratio as result of enhanced glutamate levels (Fig. 4), counterbalanced by increase of the neuronal EAAC1 and sprouting of GABAergic axon collaterals as revealed by GAD65/67 staining (Fig. 5). These changes alter the spinal homeostasis of the neuroglial network (Giaume et al., 2010) and are responsible for the synaptic disfunction following nerve injury. Intriguingly, i.t. NS delivery increases the endogenous NGF expression, restoring the expression of neuronal glutamate/glycine/GABA transporters (Fig. 3 and 5) and reducing the Glutamate/GABA ratio (Fig. 4).

Beside their active role in the homeostatic uptake of neuro/glial transmitters, astrocytes provide neurons with glutathione (GSH), one of the major neuroprotective and antioxidant systems. GSH is a tripeptide comprised of glutamate, cysteine, and glycine. It acts as a carrier/storage reservoir for cysteine and glutamate, as a neuromodulator/neurotransmitter (NMDA receptor binding) and it is required for cell proliferation and neuronal differentiation (Aoyama et al., 2008). EAAC1 plays an important role in neuronal GSH synthesis, providing neurons with cysteine (Zerangue and

342 Kavanaugh, 1996). However, GSH levels dramatically decreased despite the increased expression
343 of EAAC1 after SNI (Fig. 6), paralleled by the reactive gliosis-induced reduction of glutamate and
344 glycine transporters. The drop in GSH level might be probably due to a deficient availability of its
345 constitutive amino acids and/or to the activation of a further maladaptive mechanism using its
346 rapid turnover to obtain glutamate and enhance synaptic neurotoxicity (Sedlak et al., 2018).
347 Moreover, the relationship between GSH and the PA/plasmin system has been supposed after the
348 observation that pharmacological depletion of GSH produces a significant inhibition of the
349 PA/plasmin system (Lasierra-Cirujeda et al., 2013). tPA/PA/plasmin system blockage by i.t. delivery
350 of NS restored the expression of gluta- mate and glycine transporters and increased the GSH
351 levels. This result prompts us to hypothesize a possible mechanism for GSH homeostasis in the
352 CNS, linking together tPA/PA/plasmin system, NGF metabolism, activation of glial cells and
353 expression of glycine and glutamate transporters.

354 Besides mechanisms of impaired neuroglial synaptic plasticity and homeostasis, this work confirms
355 the active role played by blood and matrix components in regulating the levels of NGF, that in turn
356 is involved in the modulation of reactive gliosis and in maintenance of neuronal homeostasis after
357 PNI. NGF gain with i.t. NS delivery is also beneficial to SNI-induced neuropathic behavior, reducing
358 thermal hyperalgesia and mechanical allodynia, thus providing evidence for the neurotrophins
359 beyond the spinal synaptic pain processing system.

360

361 **5. CONCLUSIONS**

362 Taken together, our findings confirm that glial activation following PNI is paralleled by i) reduction
363 of glutamate and glycine uptake and perturbation of synaptic homeostasis; ii) alteration of glial
364 GSH pro- duction and neuroprotection against excitotoxicity; iii) increased proteolytic activity of
365 tPA/PA/plasmin/MMPs system. By inhibiting of tPA/ PA/plasmin system, i.t. delivery of NS lead to

an increment of endogenous NGF levels, strongly supporting the relevance of the neurotrophins in 1) modulating glial function, 2) maintaining synaptic homeostasis, 3) avoiding neuronal damage by glutamate excitotoxicity, providing the aminoacidic components (glutamate, glycine and cysteine) for GSH synthesis and 4) reducing neuropathic pain.

Altogether, these data highlight the beneficial role of NGF on reactive gliosis, spinal maladaptive plasticity, and chronic neuropathic pain, reinforcing the role of neurotrophins in promising therapeutic strategies against neurological disorders (Mitra et al., 2019).

AUTHOR STATEMENT

Assunta Virtuoso: methodology; data curation; validation; formal analysis; investigation; resources; data curation; writing - original draft preparation, Anna Maria Colangelo: methodology; validation; investigation; writing – review and editing. Sohaib Ali Korai: methodology; formal analysis; investigation; data curation; writing - original draft preparation. Sara Izzo: methodology; formal analysis; investigation; writing - original draft preparation. Antonio Todisco: methodology; formal analysis; investigation; writing - original draft preparation. Roberto Giovannoni: writing - original draft preparation; writing – review and editing. Marialuisa Lavitrano: resources; writing – review and editing; supervision, project administration. Michele Papa: conceptualization; resources; writing – review and editing; supervision, project administration; funding acquisition. Giovanni Cirillo: conceptualization; methodology; validation; formal analysis; investigation; writing - original draft preparation; writing – review and editing; visualization; supervision; project administration; funding acquisition.

DECLARATION OF COMPETING INTEREST

The authors declare that they have no known competing financial interests or personal relationships that could have appeared to influence the work reported in this paper.

ACKNOWLEDGEMENTS

This work was supported by grants from Regione Campania (L.R. N.5 Bando 2003 to MP), the Italian Minister of Research and University (PRIN 2007 to MP and to AMC; PRIN 2017-2017XJ38A4_003 to GC, ML, and MP), UNIMIB (Progetto ID 2019-ATESP-0001 and Progetto ID 2018- CONV-0056 to AV).

REFERENCES

Adorjan, I., Tyler, T., Bhaduri, A., Demharter, S., Finszter, C.K., Bako, M., Sebok, O.M., Nowakowski, T.J., Khodosevich, K., Møllgård, K., Kriegstein, A.R., Shi, L., Hoerder- Suabedissen, A., Ansorge, O., Molna´r, Z., 2019. Neuroserpin expression during human brain development and in adult brain revealed by immunohistochemistry and single cell RNA sequencing. J. Anat. 235, 543–554. https://doi.org/10.1111/ joa.12931.

Aoyama, K., Watabe, M., Nakaki, T., 2008. Regulation of neuronal glutathione synthesis. J. Pharmacol. Sci. 108, 227–238. https://doi.org/10.1254/jphs.08r01cr.

Bruno, M.A., Cuello, A.C., 2006. Activity-dependent release of precursor nerve growth factor, conversion to mature nerve growth factor, and its degradation by a protease cascade. Proc. Natl. Acad. Sci. Unit. States Am. 103, 6735–6740. https://doi.org/ 10.1073/pnas.0510645103.

Chaplan, S.R., Bach, F.W., Pogrel, J.W., Chung, J.M., Yaksh, T.L., 1994. Quantitative assessment of tactile allodynia in the rat paw. J. Neurosci. Methods 53, 55–63. https://doi.org/10.1016/0165-0270(94)90144-9.

412 Cheng, Y., Loh, Y.P., Birch, N.P., 2017. Neuroserpin attenuates H2O2-induced oxidative stress in
413 hippocampal neurons via AKT and BCL-2 signaling pathways. J. Mol. Neurosci. 61, 123–131.
414 https://doi.org/10.1007/s12031-016-0807-7.

415 Cinelli, P., Madani, R., Tsuzuki, N., Vallet, P., Arras, M., Zhao, C.N., Osterwalder, T., Rülicke, T.,
416 Sonderegger, P., 2001. Neuroserpin, a neuroprotective factor in focal ischemic stroke. Mol. Cell.
417 Neurosci. 18, 443–457. https://doi.org/10.1006/ mcne.2001.1028.

418 Cirillo, G., Bianco, M.R., Colangelo, A.M., Cavaliere, C., Daniele, D.L., Zaccaro, L., Alberghina, L.,
419 Papa, M., 2011. Reactive astrocytosis-induced perturbation of synaptic homeostasis is restored by
420 nerve growth factor. Neurobiol. Dis. 41, 630–639. https://doi.org/10.1016/j.nbd.2010.11.012.

421 Cirillo, G., Cavaliere, C., Bianco, M.R., De Simone, A., Colangelo, A.M., Sellitti, S., Alberghina, L.,
422 Papa, M., 2010. Intrathecal NGF administration reduces reactive astrocytosis and changes
423 neurotrophin receptors expression pattern in a rat model of neuropathic pain. Cell. Mol.
424 Neurobiol. 30, 51–62. https://doi.org/10.1007/s10571- 009-9430-2.

425 Cirillo, G., Colangelo, A.M., Berbenni, M., Ippolito, V.M., De Luca, C., Verdesca, F., Savarese, L.,
426 Alberghina, L., Maggio, N., Papa, M., 2015. Purinergic modulation of spinal neuroglial maladaptive
427 plasticity following peripheral nerve injury. Mol. Neurobiol. 52, 1440–1457.
428 https://doi.org/10.1007/s12035-014-8943-y.

429 Cirillo, G., Colangelo, A.M., Bianco, M.R., Cavaliere, C., Zaccaro, L., Sarmientos, P., Alberghina, L.,
430 Papa, M., 2012. BB14, a Nerve Growth Factor (NGF)-like peptide shown to be effective in reducing
431 reactive astrogliosis and restoring synaptic homeostasis in a rat model of peripheral nerve injury.
432 Biotechnol. Adv. 30, 223–232. https://doi.org/10.1016/j.biotechadv.2011.05.008.

433 Colangelo, A.M., Bianco, M.R., Vitagliano, L., Cavaliere, C., Cirillo, G., De Gioia, L., Diana, D.,
434 Colombo, D., Redaelli, C., Zaccaro, L., Morelli, G., Papa, M., Sarmientos, P., Alberghina, L.,

435 Martegani, E., 2008. A new nerve growth factor- mimetic peptide active on neuropathic pain in
436 rats. J. Neurosci. 28, 2698–2709. https://doi.org/10.1523/JNEUROSCI.5201-07.2008.

437 De Leo, J.A., Tawfik, V.L., LaCroix-Fralish, M.L., 2006. The tetrapartite synapse: path to CNS
438 sensitization and chronic pain. Pain 122, 17–21. https://doi.org/10.1016/j. pain.2006.02.034.

439 De Luca, C., Colangelo, A.M., Alberghina, L., Papa, M., 2018. Neuro-immune hemostasis:
440 homeostasis and diseases in the central nervous system. Front. Cell. Neurosci. 12, 459.
441 https://doi.org/10.3389/fncel.2018.00459.

442 De Luca, C., Papa, M., 2016. Looking inside the matrix: perineuronal nets in plasticity, maladaptive
443 plasticity and neurological disorders. Neurochem. Res. 41, 1507–1515.
444 https://doi.org/10.1007/s11064-016-1876-2.

445 Decosterd, I., Woolf, C.J., 2000. Spared nerve injury: an animal model of persistent peripheral
446 neuropathic pain. Pain 87, 149–158. https://doi.org/10.1016/S0304- 3959(00)00276-1.

447 Gelderblom, M., Neumann, M., Ludewig, P., Bernreuther, C., Krasemann, S., Arunachalam, P.,
448 Gerloff, C., Glatzel, M., Magnus, T., 2013. Deficiency in serine protease inhibitor neuroserpin
449 exacerbates ischemic brain injury by increased post ischemic inflammation. PloS One 8, e63118.
450 https://doi.org/10.1371/journal. pone.0063118.

451 Giaume, C., Koulakoff, A., RouX, L., Holcman, D., Rouach, N., 2010. Astroglial networks: a step
452 further in neuroglial and gliovascular interactions. Nat. Rev. Neurosci. 11, 87–99.
453 https://doi.org/10.1038/nrn2757.

454 Gwak, Y.S., Hulsebosch, C.E., Leem, J.W., 2017. Neuronal-glial interactions maintain chronic
455 neuropathic pain after spinal cord injury, 2017 Neural Plast. 1–14.
456 https://doi.org/10.1155/2017/2480689.

457 Hargreaves, K., Dubner, R., Brown, F., Flores, C., Joris, J., 1988. A new and sensitive method for
458 measuring thermal nociception in cutaneous hyperalgesia. Pain 32, 77–88.
459 https://doi.org/10.1016/0304-3959(88)90026-7.

460 Harrington, A.W., Leiner, B., Blechschmitt, C., Arevalo, J.C., Lee, R., Morl, K., Meyer, M.,
461 Hempstead, B.L., Yoon, S.O., Giehl, K.M., 2004. Secreted proNGF is a pathophysiological death-
462 inducing ligand after adult CNS injury. Proc. Natl. Acad. Sci. Unit. States Am. 101, 6226–6230.
463 https://doi.org/10.1073/pnas.0305755101.

464 James, M.L., Belichenko, N.P., Shuhendler, A.J., Hoehne, A., Andrews, L.E., Condon, C., Nguyen,
465 T.V.V., Reiser, V., Jones, P., Trigg, W., Rao, J., Gambhir, S.S., Longo, F.M., 2017. [18F]GE-180 PET
466 detects reduced microglia activation after LM11A-31 therapy in a mouse model of Alzheimer's
467 disease. Theranostics 7, 1422–1436. https://doi.org/10.7150/thno.17666.

468 Kement, D., Reumann, R., Schostak, K., Voß, H., Douceau, S., Dottermusch, M., Schweizer, M.,
469 Schlüter, H., Vivien, D., Glatzel, M., Galliciotti, G., 2021. Neuroserpin is strongly expressed in the
470 developing and adult mouse neocortex but its absence does not perturb cortical lamination and
471 synaptic proteome. Front. Neuroanat. 15. https://doi.org/10.3389/fnana.2021.627896.

472 Kim, W., Kim, S.K., Nabekura, J., 2017. Functional and structural plasticity in the primary
473 somatosensory cortex associated with chronic pain. J. Neurochem. 141, 499–506.
474 https://doi.org/10.1111/jnc.14012.

475 Krueger, S.R., Ghisu, G.-P., Cinelli, P., Gschwend, T.P., Osterwalder, T., Wolfer, D.P., Sonderegger,
476 P., 1997. Expression of neuroserpin, an inhibitor of tissue plasminogen activator, in the developing
477 and adult nervous system of the mouse. J. Neurosci. 17, 8984–8996.
478 https://doi.org/10.1523/JNEUROSCI.17-23-08984.1997.

479 Kuner, R., Flor, H., 2016. Structural plasticity and reorganisation in chronic pain. Nat. Rev.
480 Neurosci. 18, 20–30. https://doi.org/10.1038/nrn.2016.162.

481 Lasierra-Cirujeda, Coronel, j, Gimeno, Aza, 2013. Beta-amyloidolysis and glutathione in Alzheimer's
482 disease. Hematol. Res. Rev. 15, 31–38. https://doi.org/10.2147/jbm. s35496.

483 Lee, T.W., Tsang, V.W.K., Birch, N.P., 2015. Physiological and pathological roles of tissue
484 plasminogen activator and its inhibitor neuroserpin in the nervous system. Front. Cell. Neurosci. 9,
485 396. https://doi.org/10.3389/fncel.2015.00396.

486 Lee, T.W., Tsang, V.W.K., Loef, E.J., Birch, N.P., 2017. Physiological and pathological functions of
487 neuroserpin: regulation of cellular responses through multiple mechanisms. Semin. Cell Dev. Biol.
488 62, 152–159. https://doi.org/10.1016/j. semcdb.2016.09.007.

489 Li, W., Asakawa, T., Han, S., Xiao, B., Namba, H., Lu, C., Dong, Q., Wang, L., 2017. Neuroprotective
490 effect of neuroserpin in non-tPA-induced intracerebral hemorrhage mouse models. BMC Neurol.
491 17, 196. https://doi.org/10.1186/s12883-017-0976-1.

492 Li, Z., Liu, F., Zhang, L., Cao, Y., Shao, Y., Wang, X., Jiang, X., Chen, Z., 2018. Neuroserpin restores
493 autophagy and promotes functional recovery after acute spinal cord injury in rats. Mol. Med. Rep.
494 17, 2957–2963. https://doi.org/10.3892/ mmr.2017.8249.

495 Lo´pez-Gonza´lez, M.J., Landry, M., Favereaux, A., 2017. MicroRNA and chronic pain: from
496 mechanisms to therapeutic potential. Pharmacol. Ther. 180, 1–15.
497 https://doi.org/10.1016/j.pharmthera.2017.06.001.

498 Martorana, F., Gaglio, D., Bianco, M., Aprea, F., Virtuoso, A., Bonanomi, M., Alberghina, L., Papa,
499 M., Colangelo, A., 2018. Differentiation by nerve growth factor (NGF) involves mechanisms of
500 crosstalk between energy homeostasis and mitochondrial remodeling. Cell Death Dis. 9, 391.
501 https://doi.org/10.1038/s41419- 018-0429-9.

Merlini, M., Rafalski, V.A., Rios Coronado, P.E., Gill, T.M., Ellisman, M., Muthukumar, G., Subramanian, K.S., Ryu, J.K., Syme, C.A., Davalos, D., Seeley, W. W., Mucke, L., Nelson, R.B., Akassoglou, K., 2019. Fibrinogen induces microglia- mediated spine elimination and cognitive impairment in an alzheimer's disease model. Neuron 101, 1099–1108.e6. https://doi.org/10.1016/j.neuron.2019.01.014.

Mitra, S., Behbahani, H., Eriksdotter, M., 2019. Innovative therapy for alzheimer's disease-with focus on biodelivery of NGF. Front. Neurosci. 13, 38. https://doi.org/ 10.3389/fnins.2019.00038.

Nykjaer, A., Lee, R., Teng, K.K., Jansen, P., Madsen, P., Nielsen, M.S., Jacobsen, C., Kliemannel, M., Schwarz, E., Willnow, T.E., Hempstead, B.L., Petersen, C.M., 2004. Sortilin is essential for proNGF-induced neuronal cell death. Nature 427, 843–848. https://doi.org/10.1038/nature02319.

Osikowicz, M., Longo, G., Allard, S., Cuello, A.C., Ribeiro-da-Silva, A., 2013. Inhibition of endogenous NGF degradation induces mechanical allodynia and thermal hyperalgesia in rats. Mol. Pain 9, 37. https://doi.org/10.1186/1744-8069-9-37.

Papa, M., Canitano, A., Boscia, F., Castaldo, P., Sellitti, S., Porzig, H., Taglialatela, M., Annunziato, L., 2003. Differential expression of the Na-Ca^2 exchanger transcripts and proteins in rat brain regions. J. Comp. Neurol. 461, 31–48. https://doi.org/ 10.1002/cne.10665.

Papa, M., De Luca, C., Petta, F., Alberghina, L., Cirillo, G., 2014. Astrocyte-neuron interplay in maladaptive plasticity. Neurosci. Biobehav. Rev. 42, 35–54. https://doi.org/10.1016/j.neubiorev.2014.01.010.

Parmar, P.K., Coates, L.C., Pearson, J.F., Hill, R.M., Birch, N.P., 2002. Neuroserpin regulates neurite outgrowth in nerve growth factor-treated PC12 cells. J. Neurochem. 82, 1406–1415. https://doi.org/10.1046/j.1471-4159.2002.01100.X.

524 Reumann, R., Vierk, R., Zhou, L., Gries, F., Kraus, V., Mienert, J., Romswinkel, E., Morellini, F.,
525 Ferrer, I., Nicolini, C., Fahnestock, M., Rune, G., Glatze, M., Galliciotti, G., 2017. The serine
526 protease inhibitor neuroserpin is required for normal synaptic plasticity and regulates learning and
527 social behavior. Learn. Mem. 24, 650–659. https://doi.org/10.1101/lm.045864.117.

528 Rizzi, C., Tiberi, A., Giustizieri, M., Marrone, M.C., Gobbo, F., Carucci, N.M., Meli, G., Arisi, I.,
529 D'Onofrio, M., Marinelli, S., Capsoni, S., Cattaneo, A., 2018. NGF steers microglia toward a
530 neuroprotective phenotype. Glia 66, 1395–1416. https://doi. org/10.1002/glia.23312.

531 Sedlak, T.W., Paul, B.D., Parker, G.M., Hester, L.D., Taniguchi, Y., Kamiya, A., Snyder, S. H., Sawa,
532 A., 2018. The glutathione cycle shapes synaptic glutamate activity. Proc. Natl. Acad. Sci. Unit.
533 States Am. 3–8. https://doi.org/10.1073/pnas.1817885116.

534 Siconolfi, L.B., Seeds, N.W., 2003. Mice lacking tissue plasminogen activator and urokinase
535 plasminogen activator genes show attenuated matrix metalloproteases activity after sciatic nerve
536 crush. J. Neurosci. Res. 74, 430–434. https://doi.org/ 10.1002/jnr.10786.

537 Sofroniew, M.V., Howe, C.L., Mobley, W.C., 2002. Nerve growth factor signaling, neuroprotection,
538 and neural repair. Annu. Rev. Neurosci. 24, 1217–1281.
539 https://doi.org/10.1146/annurev.neuro.24.1.1217.

540 Virtuoso, A., De Luca, C., Gargano, F., Colangelo, A.M., Papa, M., 2020. The spinal extracellular
541 matrix modulates a multi-level Protein net and epigenetic inducers following peripheral nerve
542 injury. Neuroscience 451, 216–225. https://doi.org/ 10.1016/j.neuroscience.2020.09.051.

543 Virtuoso, A., Herrera-Rincon, C., Papa, M., Panetsos, F., 2019. Dependence of neuroprosthetic
544 stimulation on the sensory modality of the trigeminal neurons following nerve injury. Implications
545 in the design of future sensory neuroprostheses for correct perception and modulation of
546 neuropathic pain. Front. Neurosci. 13 https://doi.org/10.3389/fnins.2019.00389.

547 Wang, L., Zhang, Y., Asakawa, T., Li, W., Han, S., Li, Q., Xiao, B., Namba, H., Lu, C., Dong, Q., 2015.
548 Neuroprotective effect of neuroserpin in oxygen-glucose deprivation- and reoxygenation-treated
549 rat astrocytes in vitro. PloS One 10, e0123932. https://doi.org/10.1371/journal.pone.0123932.

550 West, S.J., Bannister, K., Dickenson, A.H., Bennett, D.L., 2015. Circuitry and plasticity of the dorsal
551 horn - toward a better understanding of neuropathic pain. Neuroscience 300, 254–275.
552 https://doi.org/10.1016/j.neuroscience.2015.05.020.

553 Yamanaka, H., Kobayashi, K., Okubo, M., Noguchi, K., 2016. Annexin A2 in primary afferents
554 contributes to neuropathic pain associated with tissue type plasminogen activator. Neuroscience
555 314, 189–199. https://doi.org/10.1016/j. neuroscience.2015.11.058.

556 Yang, X., Asakawa, T., Han, S., Liu, L., Li, W., Wu, W., Luo, Y., Cao, W., Cheng, X., Xiao, B., Namba,
557 H., Lu, C., Dong, Q., Wang, L., 2016. Neuroserpin protects rat neurons and microglia-mediated
558 inflammatory response against oxygen-glucose deprivation- and reoxygenation treatments in an in
559 vitro study. Cell. Physiol. Biochem. 38, 1472–1482. https://doi.org/10.1159/000443089.

560 Zerangue, N., Kavanaugh, M.P., 1996. Interaction of L-cysteine with a human excitatory amino acid
561 transporter. J. Physiol. 493, 419–423. https://doi.org/10.1113/ jphysiol.1996.sp021393.

562

FIGURES

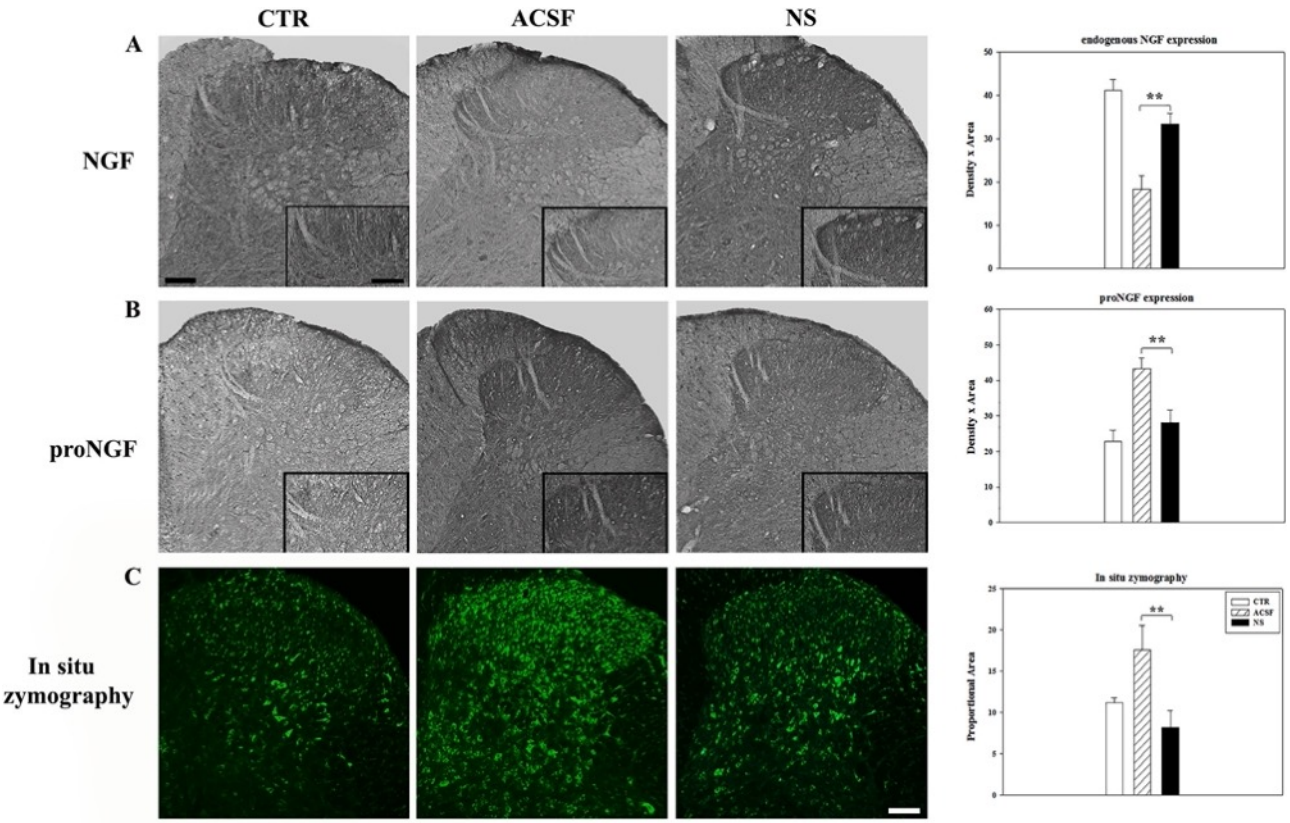

Figure 1. (A–B) Endogenous NGF and proNGF expression in the lumbar spinal cord. Sections of the dorsal horns of lumbar spinal cords from sham-operated (CTR) and SNI animals treated for 7 days with NS or ACSF and immunostained with antibodies against NGF (A) and proNGF (B). Magnification 10X, boX 20X; scale bars 500 µm. (C) In situ zymography for MMPs activity. In situ zymography for MMPs activity on sections of the dorsal horns of lumbar spinal cords from sham-operated (CTR) and SNI animals treated for 7 days with NS or ACSF. Magnification 10X; scale bar 500 µm. Data expressed as the mean ± SEM (**p ≤ 0.001, ACSF vs NS, ANOVA and Holm-Sidak test).

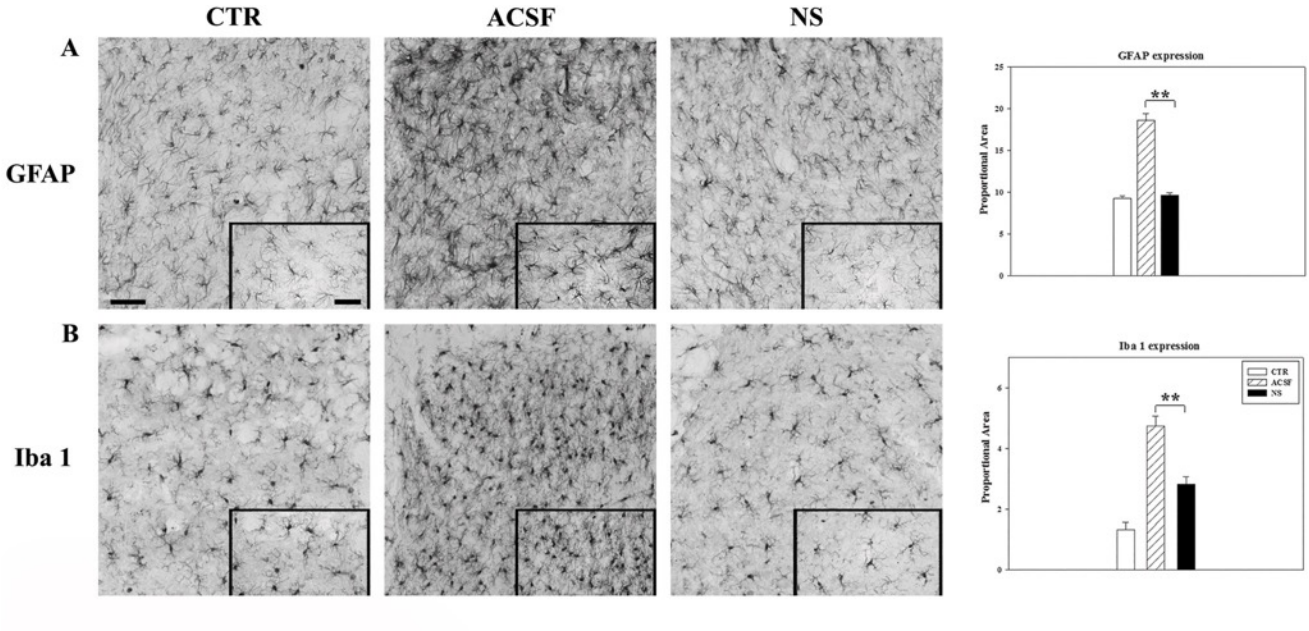

574

575 Fig. 2. Analysis of glial markers expression in the dorsal horn of the spinal cord. Sections of the
576 dorsal horns of lumbar spinal cords from sham-operated (CTR) and SNI animals treated for 7 days
577 with NS or ACSF and immunostained for GFAP (A) and Iba1 (B). Data expressed as the mean ± SEM
578 (**p ≤ 0.001, ACSF vs NS; ANOVA and Holm-Sidak test). Magnification 20X, box 40X; scale bars 500
579 µm.

580

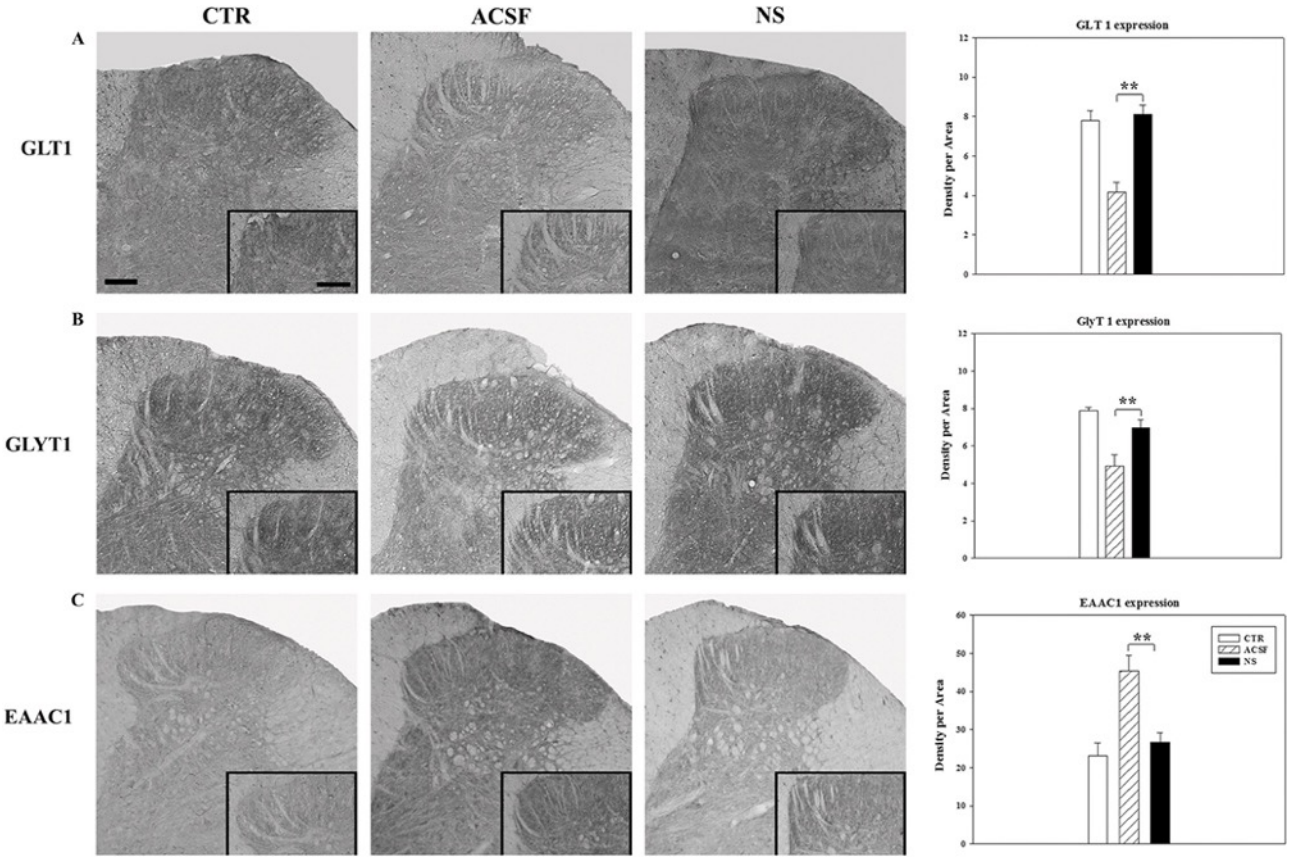

581

582 Fig. 3. Expression of neuronal and glial amino acid transporters. Sections of the dorsal horns of

583 lumbar spinal cords from sham-operated (CTR) and SNI animals treated for 7 days with NS or ACSF

584 and immunostained for GLT1 (A), GlyT1 (B) and EAAC1 (C). Data expressed as the mean ± SEM

585 (**p ≤ 0.001, ACSF vs NS; ANOVA and Holm-Sidak test). Magnification 10X, box 20X; scale bars 500

586 µm.

587

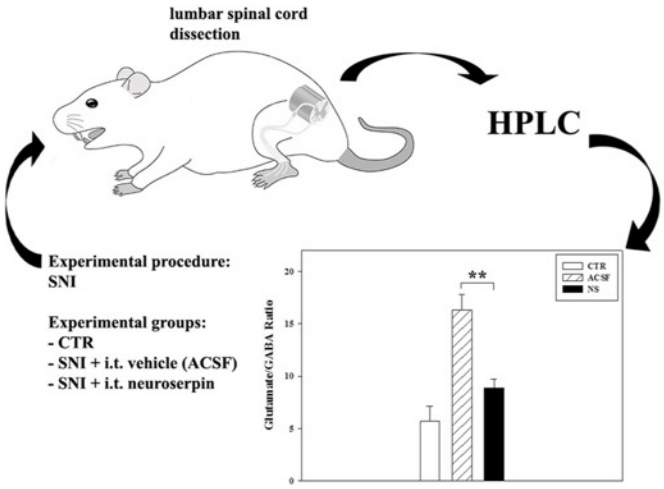

588

589 Fig. 4. Glutamate/GABA ratio. Schematic overview of HPLC analysis of amino acid levels in the

590 dorsal horns of lumbar spinal cords dissected from sham-operated (CTR) and SNI animals treated

591 for 7 days with NS or ACSF. The Glutamate/GABA ratio expressed as the mean ± SEM (**p ≤ 0.001,

592 ACSF vs NS; ANOVA and Holm-Sidak test).

593

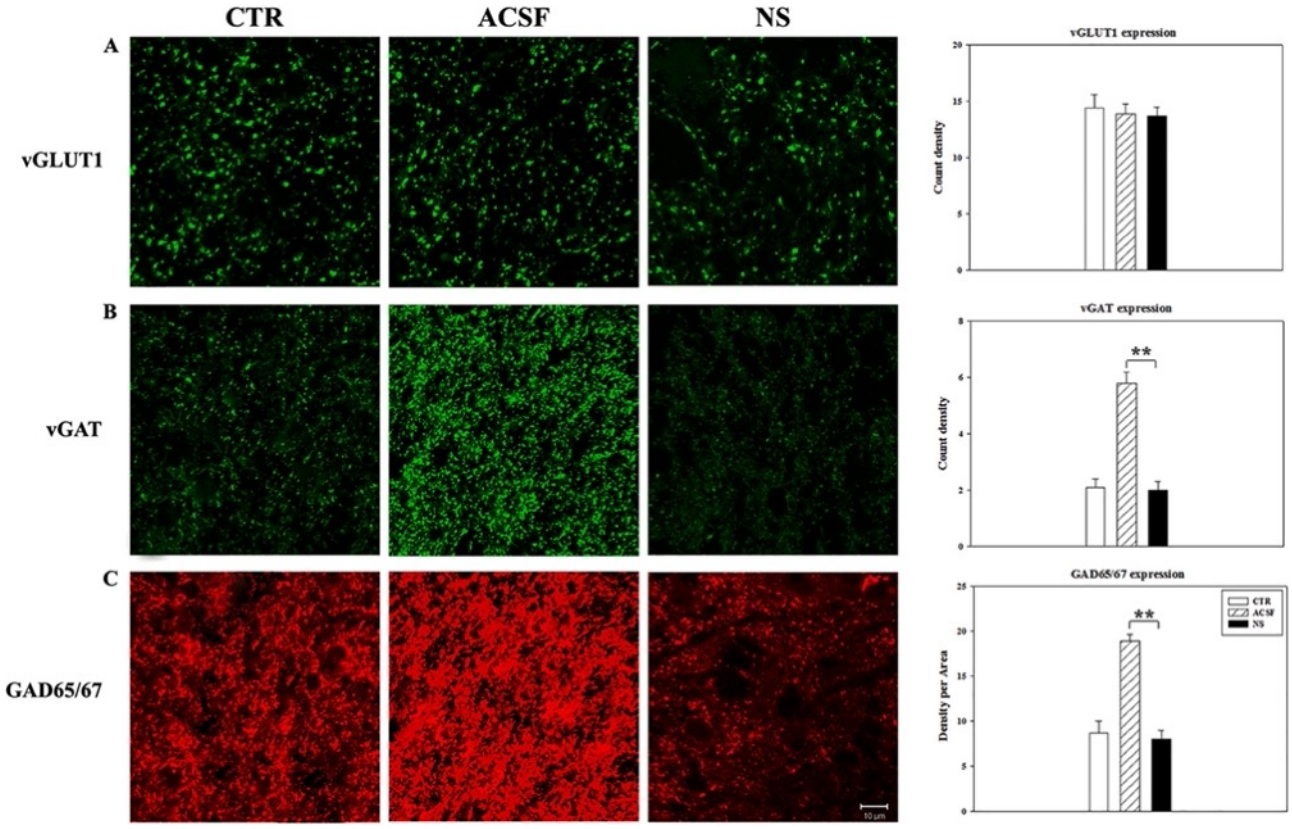

Fig. 5. Expression of vGLUT, vGAT and GAD in the dorsal horn of lumbar spinal cord. Confocal images of dorsal horns of the lumbar spinal cord immunostained for vGLUT (A), vGAT (B) and GAD (C). Sections of the dorsal horns of lumbar spinal cords from sham-operated (CTR) and SNI animals treated for 7 days with NS or ACSF. Data expressed as the mean ± SEM (**p ≤ 0.001, ACSF vs NS; ANOVA and Holm-Sidak test). Magnification 100X; scale bar 10 µm.

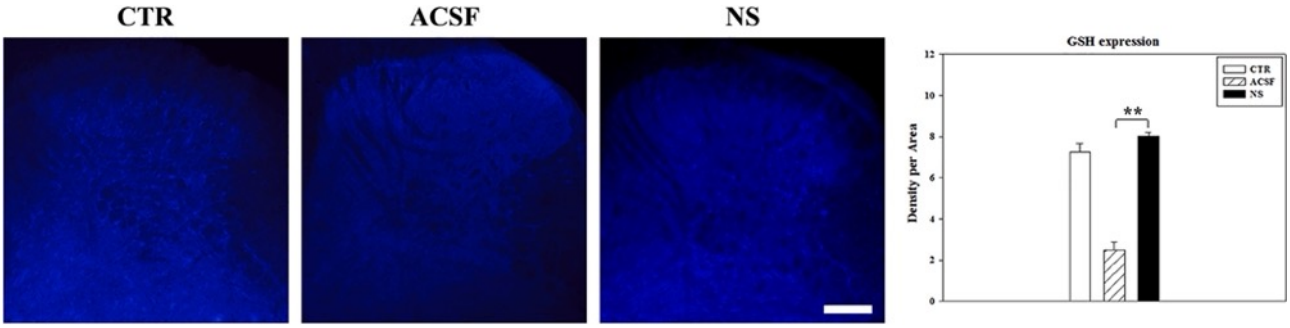

Fig. 6. GSH levels in the dorsal horn of the lumbar spinal cord. GSH levels measured in the dorsal horns of lumbar spinal cords dissected from sham-operated (CTR) and SNI animals treated for 7 days with NS or ACSF. Data expressed as the mean ± SEM (**p ≤ 0.001, ACSF vs NS; ANOVA and Holm-Sidak test). Magnification 10X; scale bar 500 µm.

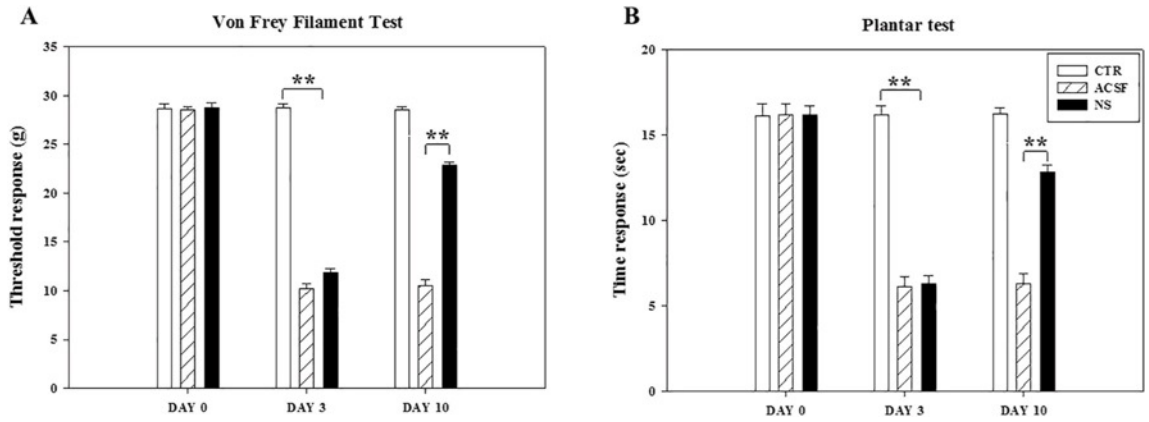

607 Fig. 7. Antinociceptive effect of i.t. administration of NS. SNI- and sham-operated rats tested for
608 responses to the von Frey (A) and the Plantar test (B) for baseline sensitivity (day 0), three days
609 after SNI (day 3) and after seven days of i.t. infusion (day 10) of NS or ACSF. Data expressed as the
610 mean ± SEM (**p ≤ 0.001, NS vs ACSF; ANOVA and Holm-Sidak test).